Chlorogenic acid combined with Epigallocatechin-3-Gallate mitigates D-galactose-induced gut aging in mice

Journal:	*Food & Function*
Manuscript ID	FO-ART-10-2022-003306.R1
Article Type:	Paper
Date Submitted by the Author:	13-Jan-2023
Complete List of Authors:	Wei, Ran; University of California Davis, Nutrition; Zhejiang Agriculture and Forestry University, Department of Tea Science Su, Zhucheng; Zhejiang Agriculture and Forestry University, Tea Science Mackenzie, Gerardo; University of California Davis, Nutrition

SCHOLARONE™
Manuscripts

1 **Chlorogenic acid combined with Epigallocatechin-3-Gallate mitigates D-**
2 **galactose-induced gut aging in mice**
3
4 Ran Wei[1], Zhucheng Su[1,*], Gerardo G. Mackenzie[2,*]
5
6 [1]Department of Tea Science, Zhejiang Agriculture and Forestry University, Hangzhou,

7 311300, China.

8 [2]Department of Nutrition, University of California, Davis, California, 95616, USA

9

10 *Corresponding authors:

11 Dr. Zhucheng Su, Ph.D.

12 Department of Tea Science, Zhejiang Agriculture and Forestry University

13 Hangzhou, Zhejiang, 311300, China

14 Phone: (0571) 63743302

15 E-mail: zhuchengsu@zafu.edu.cn

16

17 Dr. Gerardo G. Mackenzie, Ph.D.

18 Department of Nutrition, University of California, Davis

19 One Shields Ave. Davis, CA, 95616

20 Phone: (530) 752-2140; Fax: (530) 752-8966;

21 E-mail: ggmackenzie@ucdavis.edu

22

23 **Running title:** Chlorogenic acid plus EGCG ameliorates D-galactose-induced gut

24 aging

25

26

27

28

29

30

31

32

33 **Abstract**

34

35   Chlorogenic acid (CGA) and Epigallocatechin-3-Gallate (EGCG) are major

36   polyphenolic constituents of coffee and green tea with beneficial health properties. In

37   this study, we evaluated the gut protecting effect of CGA and EGCG, alone or in

38   combination, on D-galactose-induced aging mice. CGA plus EGCG more effectively

39   improved the cognition deficits and protected the gut barrier function, compared with

40   the agents alone. Specifically, CGA plus EGCG prevented the D-galactose mediated

41   reactive oxygen species accumulation by increasing the total antioxidant capacity,

42   reducing the levels of malondialdehyde, and suppressing the activity of the antioxidant

43   enzymes superoxide dismutase and catalase. In addition, supplementation of CGA

44   and EGCG suppressed gut inflammation by reducing the levels of the proinflammatory

45   cytokines TNFα, IFNγ, IL-1β and IL-6. Moreover, CGA and EGCG modulated the gut

46   microbiome altered by D-galactose. For instance, CGA plus EGCG restored the

47   Firmicutes/Bacteroidetes ratio of the aging mice to control levels. Furthermore, CGA

48   plus EGCG decreased the abundance of Lactobacillaceae, Erysipelotrichaceae, and

49   Deferribacteraceae, while increased the abundance of Lachnospiraceae,

50   Muribaculaceae, and Rikenellaceae, at the family level. In conclusion, CGA in

51   combination with EGCG ameliorated the gut alterations induced by aging, in part,

52   through antioxidant and anti-inflammatory effects, along with its gut microbiota

53   modulatory capacity.

54

55

56   **Keywords:** chlorogenic acid, EGCG, aging, oxidative stress, inflammation, microbiota

57   dysbiosis

58

59

60

61

62

63

1. Introduction

64

65   Aging is characterized by a progressive decline in individuals' adaptability,

66 physiological deterioration, and cognitive decline. Aging is also generally considered

67 as a primary risk factor for developing various diseases, such as neurodegenerative

68 disease, cardiovascular disorder, cancer, and diabetes[1]. It is estimated that in 2030,

69 one-fifth of the population will be aged older than 65, which will increase the health

70 care burden for families and governments[2]. Therefore, efforts to develop evidence-

71 based anti-aging strategies are ongoing, including genetic, drugs, specific dietary

72 interventions, and exercise.

73   Besides cognitive decline, which is a major problem during aging[3], the gut also

74 undergoes critical changes with advanced age. For example, gut barrier function

75 degenerates with aging, which plays key role in gut permeability and protecting gut

76 health[4]. Increase in oxidative stress is observed in aging and it contributes to "leaky

77 gut". Overproduction of reactive oxygen species (ROS) drives proinflammatory shift,

78 which feeds back more ROS generation. This vicious cycle causes gut dysbiosis and

79 increases gut permeability. In turn, the disruption of gut barrier facilitates translocation

80 of endotoxin, which is highly involved in initiating the low-grade inflammation[5]. Though

81 aging is an irreversible and inevitable process, the rate of aging can be controlled.

82 Studies suggest that polyphenolic compounds have potential in slowing aging. This

83 health beneficial effect is mediated, in part, by attenuating oxidative stress,

84 suppressing inflammation, preventing of telomere attrition, modulating cell apoptosis,

85 and restricting caloric intake[6].

86   Epigallocatechin-3-Gallate (EGCG) and chlorogenic acid (CGA) are the most

87 abundant and active polyphenol components present in green tea and coffee, two of

88 the most consumed beverages worldwide. For instance, a single cup of green tea

89 contains about 200-300 mg of EGCG, an amount that has been documented to have

90 health beneficial effects against various chronic diseases and aging[7]. On the other

91 hand, CGA is widely distributed in plants and accounts up to 3% (w/w) of the roasted

92 coffee powder[8]. In previous studies, EGCG and CGA have shown extensive health

93   promoting activities, such as anti-oxidation, anti-diabetes, and anti-cancer effects. In

94   addition, extensive evidence has shown that EGCG and CGA perform well in anti-

95   aging, including improving cognitive decline, relieving vascular senescence, and

96   preventing skin photoaging[9-11]. In combination, it is reported that EGCG plus CGA

97   display amplifying effect in preventing age-related bone loss, compared with each

98   agent alone[12, 13]. However, it remains unknown whether EGCG and CGA, alone or in

99   combination, could exert stronger protective effect against the aging gut.

100   In the present study, we assessed whether CGA and EGCG, alone or in

101   combination, could ameliorate gut aging induced by D-galactose. D-galactose is a

102   widely established aging model, which features cognitive dysfunction, memory loss,

103   and motor degeneration[14]. Excess accumulation of D-galactose is easily reduced and

104   catalyzed into nondegradable galactitol, which then interacts with amino acids and

105   decreases the activity of the electron transport chain. Consequently, overproduction of

106   advanced glycation end products (AGEs) and ROS accumulate with resulting

107   increased oxidative stress and inflammation[15]. Moreover, long term D-galactose

108   treatment could also damage gut integrity and lead to gut microbial dysbiosis[16]. In this

109   study, we observed that the combination of CGA and EGCG attenuates D-galactose

110   induced chronic gut injury, and this protection is mediated, in part, by their antioxidant

111   and anti-inflammatory activities as well as the modulation of the gut microbiome.

112

113   **2. Materials and Methods**

114   ***2.1 Materials and Chemicals***

115   Chlorogenic acid (purity≥98%) and EGCG (purity≥98%) were purchased from

116   Solarbio (Beijing, China). D-galactose (purity≥98%) was purchased from Aladdin

117   (Shanghai, China). The Elisa kits for TNFα, IFN-γ, IL-6 and IL-1β were purchased from

118   Multisciences Biotech (Hangzhou, China). The ReverTra Ace qPCR RT master mix

119   and the SYBR Green Realtime PCR master mix were purchased from TOYOBO

120   (Shanghai, China). The designed oligo nucleotide primers were generated by Sangon

121   Biotech (Shanghai, China). The RIPA lysis buffer, Halt protease inhibitor cocktail,

122   5×SDS-PAGE sample loading buffer, BSA, Bradford protein assay kit and ECL Plus

123   Ultra-Sensitive kit were purchased from Phygene (Haixi, China). The PVDF

124   membranes and the fluorescein isothiocyanate-dextran (FITC-Dextran) were

125   purchased from MilliporeSigma (Burlington, MA, USA). The endotoxin quantitation kit,

126   the prestained protein ladder, and the TRIzol™ Reagent were purchased from Thermo

127   Fisher Scientific (Waltham, MA, USA). The occludin (Cat#13409), claudin 1

128   (Cat#13050), zo-1 (Cat#21773) and β-actin (Cat# 20536) antibodies were purchased

129   from Proteintech™ (Wuhan, China). The total antioxidant capacity (T-AOC) assay kit,

130   malondialdehyde (MDA) colorimetric assay kit, catalase (CAT) colorimetric assay kit,

131   and superoxide dismutase (SOD) colorimetric assay kit were purchased from

132   JianCheng Bioengineering Institute (Nanjing, China).

133

134   ***2.2 Animal Studies***

135   All animal procedures were performed following the institutional and national

136   guidelines for the care and use of laboratory animals and were approved by the

137   Institutional Animal Ethics Committee at Zhejiang Agriculture and Forestry University.

138   Eight weeks old ICR female mice were purchased from Shanghai SLAC Laboratory

139   Animal Company (Shanghai, China), maintained under 12 h light cycle, semi-specific

140   pathogen-free conditions, and fed with autoclaved chow diet. Briefly, after 2 weeks

141   adaptation, mice (n=8 per group) were randomized into 5 groups: Control group (Ctrl),

142   D-galactose treated group (M), D-galactose treated group gavaged with chlorogenic

143   acid (C), D-galactose group gavaged with EGCG (E), and D-galactose group gavaged

144   with chlorogenic acid plus EGCG (C+E). Mice in D-galactose-treated groups were

145   injected intraperitoneally with 200 mg/kg/d D-galactose once per day for totally eight

146   weeks, while mice in the control group were injected with same volume of PBS instead.

147   Mice in C, E, and C+E groups were orally gavaged with 20 mg/kg/d chlorogenic acid

148   (C), 20 mg/kg/d EGCG (E), or 20 mg/kg/d chlorogenic acid plus 20 mg/kg/d EGCG

149   (C+E), dissolved in water, once daily during the whole intervention period. Meanwhile,

150   mice in the Ctrl group or the model group were gavaged with same volume of water.

151   Body weight was measured and recorded every week. Behavior tests were performed

152   during the last week before euthanasia, and fresh feces for microbiota analysis were

153   collected on the last day and stored at -80°C.Following feces collection, mice were

154   fasted 4 h for the gut permeability analysis. At the end of the experimental period, mice

155   were euthanized, blood was collected by cardiac puncture, and the brain and colon

156   (excluding caecum) tissues were carefully dissected, luminal content removed, and

157   washed with PBS. Then, samples used for RNA extractions was processed

158   immediately, samples used for histochemistry analysis was immersed in 4% (w/v)

159   paraformaldehyde for histochemistry analysis, and the remaining tissues were stored

160   at -80°C.

161

162   **2.3 Behavior tests**

163   **2.3.1 Open field test (OFT)**

164   The OFT was performed as previous described with minor modifications[17].

165   Mice were placed in the center of a white acrylic box (40cm x 40cm) with grids at the

166   bottom and allowed to move freely for 10 minutes. The behavior and moving path were

167   recorded by a top camera. Crosses mice passed through were calculated. Ethanol (70%

168   v/v) was used to clean all the objects and chamber between trials.

169   **2.3.2 Novel object recognition (NOR)**

170   The NOR test was conducted as previously described with minor

171   modifications[18]. Before testing, mice were placed in an empty open chamber in turns,

172   allowed moving freely and acclimated to the environment for 1 hour on the first day.

173   On the second day, two identical objects (object A) were put at the ends of the chamber

174   opposite to each other. Mice were given 10 minutes to adapt to the objects. On the

175   third day, one of the objects was replaced by a new one (object B), and mice were put

176   inside again for another 10 minutes to explore. The preferential index was calculated

177   using the following formula: Preferential index=Time on object B/(Time on object

178   B+Time on object A)×100%. Ethanol (70% v/v) was used to clean all the objects and

179   chamber between trials.

180

181   **2.4 Gut permeability analysis and measurement of serum endotoxin**

182   During the last day before euthanasia, mice were fasted for 4h, and then

183   gavaged with fluorescein isothiocyanate conjugated dextran (50 mg per 100 g body

184   weight)[19]. Two hours later, blood was collected and serum was obtained. Fluorescence

185   intensity (excitation, 490nm; emission, 520nm) in the serum of samples was measured

186   using the Synergy H1 microplate reader (Biotek, VT, USA).

187   Endotoxemia was determined in serum, according to the manufacturers'

188   instructions (Thermo Fisher Scientific, MA, USA). The absorbance was measured

189   using the Synergy H1 microplate reader (Biotek, VT, USA).

190

191   *2.5 Histological analysis*

192   After fixing in the 4% paraformaldehyde overnight, colon or brain samples were

193   embedded, with the paraffin embedding machine (EC350, Thermo Fisher Scientific,

194   MA, USA), sliced (4 μm) and stained with the hematoxylin and eosin (H&E). Then once

195   slices were thoroughly dried, samples were observed and representative images at

196   100x and 400x were taken with the microscopy (BX-41, Olympus, Tokyo, Japan).

197

198   *2.6 Western Blot*

199   Colon samples were homogenized and lysed with RIPA lysis buffer over ice.

200   The Bradford protein assay kit was used to test the protein content. Protein samples

201   were separated with the 4-12% gradient polyacrylamide gel electrophoresis, and then

202   transferred to the PVDF membranes. After blocking with skim milk for 1 hour, the

203   membranes were incubated with the primary antibody (zo-1, occludin and claudin 1)

204   at 4℃ overnight. β-actin was used as the loading control. After incubation with the

205   secondary antibody (HRP-conjugated; 1:2000 dilution) for 1 h, at room temperature,

206   the conjugates were developed and visualized by the 5200 Multi system (Tanon,

207   Shanghai, China).

208

209   *2.7 ELISA*

210   Colon samples were homogenized, centrifuged, and then the supernatants

211   were collected. The levels of TNFα, IFN-γ, IL-6 and IL-1β were analyzed according to

212   the manufacturers' instructions (Multisciences Biotech, Hangzhou, China), and

213 normalized by the protein levels tested by Bradford assay. The absorbance was

214 measured using the Synergy H1 microplate reader (Biotek, VT, USA).

215

216 **2.8 RNA extraction and qRT-PCR analysis**

217 Total RNA of fresh colon or brain samples were extracted using TRIzol™

218 reagent. The quality and quantity of RNA were analyzed by the Nanodrop™ One

219 spectrophotometer (Thermo Fisher Scientific, MA, USA). Afterwards, cDNA was

220 generated with the ReverTra Ace qPCR RT master mix kit by the Veriti thermal cycler

221 (Thermo Fisher Scientific, MA, USA) and stored in -80℃. The cDNA was next mixed

222 with specific primers (Table 1) and SYBR Green Realtime PCR master mix to run the

223 quantitative real-time PCR by the StepOne Realtime PCR system (Thermo Fisher

224 Scientific, MA, USA)[19-21]. Relative mRNA expression levels of specific genes were

225 calculated by the $2^{-\Delta\Delta CT}$ method and β-actin was used as a control.

226 Table 1. Primer sequences for qRT-PCR analysis

Gene name	Forward (5′-3′)	Reverse (5′-3′)
p16	CGGGGACATCAAGACATCGT	GCCGGATTTAGCTCTGCTCT
p21	CTGTCTTGCACTCTGGTGTCT	CTAAGGCCGAAGATGGGGAA
zo-1	TCTTGCTGGCCCTAAACCTG	GTTGGGCTGGCTCTGAGAAT
occludin	TTCAGGTGAATGGGTCACCG	AGATAAGCGAACCTGCCGAG
claudin 1	TGGGGCTGATCGCAATCTTT	CACTAATGTCGCCAGACCTGA
β-actin	ATGCTCTCCCTCACGCCATC	GAGGAAGAGGATGCGGCAGT

227

228 **2.9 Redox status analysis**

229 Colon samples were homogenized, centrifuged, and the supernatants were

230 collected. Supernatants were then analyzed with the T-AOC, MDA, CAT, and SOD kits

231 following the manufacturers' instructions (Jiancheng Bioengineering Institute, Nanjing,

232 China). Redox status levels were normalized by the protein levels measured by

233 Bradford assay. The absorbance was measured using the Synergy H1 microplate

234 reader (Biotek, VT, USA).

235

2.10 Gut microbe 16S rRNA sequencing

236   Microbial DNA samples were isolated from mouse feces using the E.Z.N.A.®

238   Soil DNA Kit following the manufactures' instructions (Omega Bio-tek, GA, USA). The

239   DNA   concentration   were   quantified   using   the   NanoDrop   2000   UV-vis

240   spectrophotometer (Thermo Fisher Scientific, MA, USA), and DNA quality was

241   checked by 1% agarose gel electrophoresis. Then the V3–V4 regions of bacterial 16S

242   rRNA   gene   was   amplified   with   universal   primers   338   F   (5′-

243   ACTCCTACGGGAGGCAGCAG-3′) and 806R (5′-GGACTACHVGGGTWTCTAAT-3′)

244   by ABI GeneAmp® PCR (Thermo Fisher Scientific, MA, USA). Next, the resulted PCR

245   products were extracted from a 2% (w/v) agarose gel and purified using the AxyPrep

246   DNA Gel Extraction Kit (Axygen Biosciences, CA, USA) and quantified using

247   QuantiFluor™-ST (Promega, WI, USA). Purified amplicons were then sequenced by

248   an Illumina MiSeq platform (Illumina, SD, USA) according to the standard protocols by

249   Majorbio Bio-Pharm Technology Co. Ltd. (Shanghai, China).

250

2.11 Bioinformatic analysis

252   Raw fastq files were quality-filtered by Trimmomatic and merged by FLASH.

253   Then the high-quality sequences were clustered into operational taxonomic units

254   (OTUs) according to a 97% similarity cutoff using the UPARSE (version 7.1

255   http://drive5.com/uparse/) with a novel "greedy" algorithm that performs chimera

256   filtering and OTU clustering simultaneously. The taxonomy of each 16S rRNA gene

257   sequence was analyzed by RDP Classifier algorithm (http://rdp.cme.msu.edu/).

258

2.12 Statistical analysis

260   Data was summarized as Mean±SD. SPSS (20.0 software, Chicago, IL) was

261   performed to analyze statistical differences among groups by the one-way analysis of

262   variance (ANOVA) and Turkey post hoc tests. p values<0.05 was regarded as being

263   significant different and labeled as *.

264   For the microbiota analysis, alpha diversity analysis was evaluated with the

265   standard metrics (e.g Chao, Ace, Simpson and Shannon index). The beta diversity

266   analysis was processed by the principal co-ordinates analysis (PCoA) based on the

267   Bray_Curtis distance metric method. Linear discriminant analysis effect size (LEfSe)

268   analysis was performed with the non-parametric factorial Kruskal-Wallis sum-rank test

269   and linear discriminant analysis (LDA).

270

271

272   **3. Results**

273   *3.1 Chlorogenic acid and EGCG show no toxicity in D-galactose-induced aging*

274   *mice.*

275   To evaluate the effect of CGA and EGCG on D-galactose-induced aging mice,

276   we initially assessed body weight progression and food intake every week. At the end

277   of the treatment, the body weight gain of mice treated with D-galactose [the model

278   group (M)] markedly decreased ($p<0.01$), compared with the vehicle treated control

279   group (Figure 1a). While CGA or EGCG, alone, was not able to mitigate the reduction

280   in body weight gain induced by D-galactose, CGA plus EGCG effectively recovered

281   the body weight gain to control level ($p<0.05$). Regarding food intake, the levels of it

282   decreased in all groups in the 2nd week, while it gradually recovered in the following

283   weeks, and no significant differences were observed among groups (Figure 1b).

284   To determine whether CGA and EGCG treatment affected normal liver function,

285   we assessed the levels of aminotransferases [aspartate aminotransferase (AST) and

286   alanine aminotransferase (ALT)] in serum. After eight weeks of treatment, mice in all

287   groups showed levels of these liver enzymes within the physiological ranges, with no

288   significant differences among groups (Figure 1c).

289

290   *3.2 Chlorogenic acid in combination with EGCG improves D-galactose-induced*

291   *cognitive impairment of the aging mice.*

292   We next assessed whether CGA and EGCG could improve the moving and

293   cognitive performance of aging mice (Figure 2a). In the open-field test (OFT), relative

294   to the control group (242 crosses), D-galactose decreased the crossing numbers to

295   158 crosses (p<0.05). While CGA or EGCG alone did not significantly improved on the

296   moving capacity (202 crosses and 180 crosses, respectively), CGA plus EGCG group

297   effectively recovered the moving ability (271 crosses), being significantly higher than

298   the D-galactose group (p<0.01).

299   Mice in the model group (M) also showed weaker capability on the novel object

300   recognition (NOR), with a preference index of 25.7±8.2%, which was significantly lower

301   than the control group (47.2±3.9%, p<0.01). Treatment with EGCG alone or CGA plus

302   EGCG significantly improved the preference index to 45.0±7.1% and 45.7±9.1%,

303   respectively, compared to the D-galactose group(p<0.05).

304   Next, we used H&E staining to evaluate the effect of CGA and EGCG on the

305   histopathological changes in the brain after D-galactose in the aging mice (Figure 2b).

306   The morphology of neurons stained with H&E in the control group was normal, with

307   neurons presenting around or oval and clear nucleolus with a regular arrangement. In

308   contrast, the D-galactose-treated group demonstrated severe neuronal changes, such

309   as the presence of dark pycnotic nuclei and a decrease in the cytoplasm.

310   Administration of CGA, EGCG or CGA plus EGCG mitigated this pathologic change

311   (Figure 2b).

312   Furthermore, D-galactose markedly upregulated the mRNA level of p16 and

313   p21 (p<0.05) in the brain, two key age-associated genes, compared with the control

314   group (Figure 2c). CGA and EGCG abrogated the effects of D-galactose on p16 and

315   p21, though no significant difference was observed between D-galactose group and

316   CGA, EGCG groups on p16 expression.

317

318   **_3.3 Chlorogenic acid in combination with EGCG protects the gut barrier of the_**

319   **_aging mice._**

320   To assess the effect of CGA and EGCG, alone and in combination, at the gut

321   levels of the aging mice, the colon morphology and gut permeability were evaluated.

322   As shown in Figure 3a, after eight weeks of treatment, D-galactose damaged the colon

323   structure and induced infiltration of lymphocytes in the colon region, which was

324   effectively improved by CGA and EGCG.

325 In addition, D-galactose severely damaged the gut barrier permeability (Figure

326 3b). The level of FITC-Dex transport was almost 1.8 times higher in the model group

327 than in the control group (p<0.01). Compared with D-galactose-treated mice, EGCG

328 alone and CGA plus EGCG significantly decreased the gut permeability, recovering

329 the gut permeability to normal levels (p<0.01). Consistently, higher level of serum

330 endotoxin was observed in the D-galactose treated group, compared to the control

331 group (p<0.05), and supplementation with CGA and EGCG improved the endotoxemia

332 induced by D-galactose (Figure 3c).

333 Tight Junctions (TJs) proteins play pivotal roles in controlling the gut

334 permeability. D-galactose treatment remarkably reduced the protein expression levels

335 of zo-1, occludin and claudin 1, compared to control group (p<0.01). While CGA and

336 EGCG alone were unable to restore the levels of zo-1, occludin and claudin 1, the

337 combination of CGA and EGCG effectively restored the levels of these TJs protein

338 expression to similar levels observed in control treated mice (Figure 3d). In agreement,

339 treatment with D-galactose significantly reduced mRNA expression levels of occludin

340 and claudin 1 (p<0.05), but not zo-1, which were markedly reversed by C plus E

341 treatment (p<0.01; Figure 3e).

342

343 **3.4 Chlorogenic acid in combination with EGCG reduces D-galactose-induced**

344 **colon inflammation in aging mice.**

345 We next assessed the effect of C plus E on the gut inflammation induced by D-

346 galactose (Figure 4a). In the model group, D-galactose markedly increased the levels

347 of TNFα and IL-6, compared to the control group (p<0.05). While CGA and EGCG

348 alone were unable to suppress TNFα and IL-6 levels, combination of CGA and EGCG

349 significantly reduced TNFα and IL-6 levels, compared to D-galactose alone group

350 (p<0.05). Moreover, the level of IFN-γ was enhanced to 3907.8±672.9 pg/mg prot in

351 D-galactose-treated group, whereas EGCG alone and CGA plus EGCG decreased the

352 level to 2829.9±381.3 pg/mg prot (p<0.05) and 2308.8±802.4 pg/mg prot (p<0.01),

353 respectively. Finally, compared to the control group, D-galactose also increased the

354 levels of the IL-1β to 1182.5±102.9 pg/mg prot (p<0.01). C and E both alone or in

355   combination decreased the IL-1β secretion as compared to model group (p<0.01).

356

3.5 Chlorogenic acid in combination with EGCG decreases D-galactose-induced

357

358   **_colon oxidative stress in aging mice._**

359   Oxidative stress is another main factor contributing to the enhanced gut

360   permeability. As shown in Figure 4b, compared to control mice, D-galactose

361   significantly decreased the level of total antioxidant capacity (T-AOC) by 29% (p<0.05),

362   and induced a 2-fold increase in MDA levels (p<0.05). The pro-oxidative effect of D-

363   galactose was reversed by the combination of CGA and EGCG. Aging mice treated

364   with CGA plus EGCG displayed significantly higher level of T-AOC capacity and lower

365   level of MDA compared to D-galactose treated mice (p<0.05). Moreover, the activities

366   of catalase (CAT) and superoxide dismutase (SOD) were also reduced (p<0.05) in the

367   model group, compared to controls. CGA and EGCG alone partly recovered CAT and

368   SOD activities, whereas CGA plus EGCG greatly increased the SOD activity (p<0.05).

369

3.6 Chlorogenic acid in combination with EGCG improves D-galactose-induced

370

371   **_gut dysbiosis in aging mice._**

372   16S rRNA sequencing was performed to evaluate taxa with differential

373   abundance between the aging mice and the ones treated with CGA and EGCG.

374   Compared to the control group, mice in the D-galactose-treated group exhibited overall

375   lower alpha diversity (Figure 5). In the model group, the Shannon index decreased to

376   3.5 (p<0.01) and the Simpson index increased to 0.1 (p<0.01), two main factors

377   representing the community diversity. CGA alone recovered the Shannon index to 4.1

378   (p<0.05), and its effect was strengthened when combined with EGCG (p<0.01).

379   Similarly, CGA plus EGCG significantly decreased the Simpson index, compared with

380   the model group (p<0.01). As the Ace index and Chao index shown, the community

381   richness of aging mice was also decreased, and only C plus E could effectively recover

382   the community richness to the normal level (p<0.05).

383   We next analyzed the species diversity among groups on OTU level. Notably,

384   control and CGA plus EGCG groups shared similarities in PCoA, while the other three

385   groups were quite far away, suggesting that the combination of CGA plus EGCG has

386   a stronger effect in modulating gut dysbiosis than either agent alone (Figure 6a).

387   Then the community abundance on phylum level and family level were

388   analyzed, respectively. As shown in Figure 6b, compared to the control group, the ratio

389   of Firmicutes, Deferribacter, Actinobacter, and Proteobacter increased, while the ratio

390   of Bacteroidota, Desulfobacte, and Campilobacte decreased in the model group,

391   indicating gut dysbiosis occurred in the aging mice. Compared with the control group,

392   the ratio of Firmicutes/Bacteroidetes in the D-galactose group significantly increased

393   to 3.3±1.6 (p<0.05). Both CGA and EGCG positively modulated the gut dysbiosis and

394   showed better effects when combined. The ratio of Firmicutes/Bacteroidetes

395   decreased to 1.0±0.7 in the CGA plus EGCG group, significantly lower than the model

396   group (p<0.01). Furthermore, as shown in Figure 6c, the community abundance on

397   family level was further analyzed. Compared to the control group, the level of

398   Lactobacillaceae,   Erysipelotrichaceae,   Deferribacteraceae,   Sutterellaceae,

399   Bifidobacteriaceae, and Eggerthellaceae increased in the model group, while the level

400   of Lachnospiraceae,   Muribaculaceae,   Rikenellaceae,   Bacteroidaceae,   and

401   Prevotellaceae decreased. Though CGA and EGCG alone were unable to show a

402   strong effect on D-galactose induced microbiota alteration, CGA plus EGCG greatly

403   affected the microbiota, and the level of Lactobacillaceae was sharply decreased and

404   the ratio of Lachnospiraceae, Muribaculaceae, and Rikenellaceae increased. At the

405   genus level, the top 50 genera with highest community abundance were selected. The

406   relative abundance of dominant genera in the control group and CGA plus EGCG

407   group are relatively similar, while no significant differences were detected among the

408   D-galactose group, CGA group or EGCG group (Figure 6d).

409   In Figure 7, the dominant microbiota among groups were analyzed by the

410   LEfSe (LDA＞2). In the control group, there are totally 13 prominent features, includes

411   *g_Alistipes   g_Ruminococcus*,   and   *g_Anaeroplasma*,   whereas   c_Bacilli,

412   *o_Lactobacillales*, p_Firmicutes and *o_Enterobacterales*, etc are the 12 specific taxa

413   found in the model group. After CGA plus EGCG treatment, 12 key phylotypes were

414   identified,   includes   *o_Bacteroidales*,   *g_Candidatus_Soleaferrea*,

415   *o_unclassified_c_Clostridia,*   *g_unclassfied_f_Anaerovoracaceae,*

416   *g_unclassified_f_Prevotellaceae*, and *g_Tuzzerella*.

417

418   **4. Discussion**

419   In the present study, we evaluated the anti-aging impact of EGCG and CGA,

420   alone or in combination, with a particular focus on the effect at the gut level. While

421   EGCG and CGA alone partly improve the aging process induced by D-galactose, a

422   significant better effect was observed when these two bioactives were combined.

423   Cognitive degeneration is a major pathology during aging[3]. In agreement with

424   other studies, the current results showed that chronic administration of D-galactose

425   causes deleterious neuronal damage, which was prevented by CGA and EGCG[22, 23].

426   Multiple pathways involved in the regulation of aging, particularly, increased

427   expression of p16 and p21 are crucial markers[21]. Though less obvious than brain

428   degeneration, gut also undergoes critical changes during aging with gut permeability

429   increased. Here, D-galactose treatment increased the gut permeability with higher

430   level of serum endotoxin observed. EGCG plus CGA prevented the endotoxemia

431   induced by D-galactose and protected the impaired gut barrier. Mechanistically, TJ

432   proteins connect intercellularly and work as physical barrier in regulating gut

433   permeability[24]. We observed that the combination of CGA and EGCG protected TJs,

434   including zo-1, occludin, and claudin 1, which were damaged by the D-galactose

435   Aging-dependent gut impairment is linked to chronic oxidative stress, low-

436   grade inflammation and alterations in gut microbiome[25]. Gut highly relies on

437   mitochondrial oxidative phosphorylation (OXPHOS) to meet its high energy

438   requirements, thus it is more susceptible to oxidative injury. Therefore, oxidative stress

439   is widely recognized as the main inductive factor for accelerating gut aging. Due to

440   their antioxidant capacity, CGA and EGCG maintained gut redox balance.

441   Administration of CGA plus EGCG has a stronger effect in attenuating oxidative stress

442   by further increasing the activity of CAT and SOD and decreasing the level of MDA,

443   compared with either agent alone.

444   Most aged individuals develop a mild proinflammatory state, which is related to

445   increased susceptibility to multiple age-related diseases. The chronic progressive

446   inflammatory process with age was regarded as "inflamm-aging"[26]. Under such a state,

447   levels of pro-inflammatory cytokines markedly elevate and promote the disruption of

448   gut epithelial barriers[27]. Evidence showed that proinflammatory cytokines TNFα, IFNγ,

449   IL-1β and IL-6 play crucial role in the inflammation amplification cascade, contributing

450   greatly in causing functional opening of TJ barrier[28]. In the present study, D-galactose

451   exposure increased TNFα, IFN-γ, IL-6 and IL-1β levels, which was suppressed by CGA

452   plus EGCG.

453   Microbiota profile undergoes alterations with increasing age, which affects the

454   gut barrier function and modulates the cognitive capacity through gut-brain axis. In

455   general, Firmicutes and Bacteroidota are the most represented bacteria in all groups,

456   accounting for up to 80% of the total microbiota[29]. The Firmicutes/Bacteroidota ratio

457   evolves during different life stages. Treatment with D-galactose upregulated ratio of

458   Firmicutes/Bacteroidota, which is consistent with other studies[30]. Higher contribution

459   of Deferribacterota was also observed in the D-galactose treated mice, which was

460   positively relevant to gut inflammation[31, 32]. Besides, these shifts were accompanied by

461   an increased prevalence of Actinobacteriota and Proteobacteria, and a reduction in

462   Desulfobacterota in the D-galactose group, which is in line with previous studies[30, 33].

463   CGA and EGCG reversed the microbial shift induced by D-galactose, and better effect

464   was observed when these two drugs were combined.

465   At family taxonomic level, treatment with D-galactose increased the level of

466   Lactobacillaceae and decreased the abundance of Lachnospiraceae, and these

467   changes were effectively prevented by CGA plus EGCG. Lactobacillaceae is one of

468   the essential bacteria promotes the growth of secondary bile acids, and highly enriched

469   in the ileum of aging rats[34]. It is observed that Lactobacillaceae could robustly acidify

470   the environment, and inhibit the growth of the commensal gut bacteria, such as

471   Lachnospiraceae and Muribaculaceae (S24-7)[35]. Lachnospiraceae positively

472   modulates the gut barrier integrity and maintains the gut permeability in aged mice[36].

473   In addition, CGA and EGCG improved the levels of Muribaculaceae, Rikenellaceae,

474   and Bacteroidaceae, which were reduced by D-galactose. Previous studies

475　demonstrated that compared with the young ones, aged mice displayed lower level of

476　Muribaculaceae (S24-7), which is positively associated with gut health and longevity

477　of mice by producing short chain fatty acids, in particular, propionate[37]. High amount

478　of Rikenellaceae is associated with healthy aging and longevity in Italian elderly and

479　related with lower risk of metabolic diseases[38]. Moreover, during neonatal dairy calves

480　aging, a decreased abundance of Bacteroidaceae was found to be one of the

481　predominant alterations in the fecal microbiome composition[39]. It is worth noting that

482　CGA plus EGCG treatment protected against the overgrowth of Erysipelotrichaceae

483　and Deferribacteraceae, which are positively correlated with inflammation-related

484　gastrointestinal diseases, such as colorectal cancer, inflammatory bowel disease (IBD)

485　and Crohn's disease (CD)[31, 40]

486　　　　Moreover, the key phylotypes from phylum to genus of Ctrl, M and C plus E

487　group were identified. c_Bacilli (phylum Firmicutes) was found highly enriched in the

488　model group, and similar results were found in elderly adults[41]. f_Enterobacteriaceae

489　(phylum Proteobacteria) enrichment is frequently coincidence with considerable gut

490　pathology. Patients with inflammatory bowel disease exhibited higher abundance of

491　Enterobacteriaceae, and the outgrowth of Enterobacteriaceae could reversely result in

492　gastrointestinal cell apoptosis and inflammation[42-44]. The abundance of *g_Escherichia-*

493　*Shigella* was positively correlated with the blood levels of pro-inflammatory cytokines,

494　and could promote the secretion of endotoxins. In CGA plus EGCG supplementation

495　group, *g_Candidatus_Soleaferrea* genus was identified as one of the key taxons

496　possessing anti-inflammatory capacity and maintaining the gut homeostasis[45].

497　f_Anaerovoracaceae was sparsely characterized, and it was reported to be involved

498　in the gut digestion of plant polyphenols[46]. f_Prevotellaceae enhances SCFAs

499　production, and could protect the gut barrier integrity and improve gut microbiota

500　dysbiosis[47]. In Alzheimer's disease patients, c_Clostridia and *g_Tuzzerella* were

501　characterized by a decreased amount[48].

502

503　**5.　Conclusion**

504　　　　CGA plus EGCG exerts stronger protective effects against aging related gut

505   barrier impairment than CGA or EGCG alone. After challenged with D-galactose, CGA

506   plus EGCG effectively improved the redox status and mitigated the gut inflammation

507   damage of the aging mice. Moreover, CGA plus EGCG attenuated the gut homeostasis

508   disturbed by D-galactose, which is characterized by a reduced community diversity

509   and microbiome shift. A limitation of this study is that it evaluated the combined effect of

510   the CGA and EGCG against each compound alone at single doses. An important question

511   that needs clarification is whether the stronger protective aging-related gut barrier effects

512   observed with CGA plus EGCG is due to an additive effect between these agents or

513   whether it might be simply due to the presence of higher doses of beneficial compounds

514   at the gut level. Future studies are warranted to elucidate whether CGA and EGCG

515   sensitize each other and whether the combined effect of CGA plus EGCG is superior than

516   a higher dose of the individual compounds. Taken together, these results suggest that

517   the combination of CGA and EGCG is safe and effective in improving the gut barrier

518   function during the aging process.

519

520

521

522

523

524   **Conflicts of Interest**: The authors declare no conflict of interest.

525

530

531

532

References

533

534   1.   L. Partridge, J. Deelen and P. E. Slagboom, Facing up to the global challenges of ageing, *Nature*,
535   2018, **561**, 45-56.
536   2.   P. A. Heidenreich, J. G. Trogdon, O. A. Khavjou, J. Butler, K. Dracup, M. D. Ezekowitz, E. A.
537   Finkelstein, Y. Hong, S. C. Johnston, A. Khera, D. M. Lloyd-Jones, S. A. Nelson, G. Nichol, D.
538   Orenstein, P. W. Wilson, Y. J. Woo, C. American Heart Association Advocacy Coordinating, C.
539   Stroke, R. Council on Cardiovascular, Intervention, C. Council on Clinical, E. Council on,
540   Prevention, A. Council on, Thrombosis, B. Vascular, C. Council on, C. Critical, Perioperative,
541   Resuscitation, N. Council on Cardiovascular, D. Council on the Kidney in Cardiovascular, S.
542   Council on Cardiovascular, Anesthesia, C. Interdisciplinary Council on Quality of and R.
543   Outcomes, Forecasting the future of cardiovascular disease in the United States: a policy
544   statement from the American Heart Association, *Circulation*, 2011, **123**, 933-944.
545   3.   K. F. Azman and R. Zakaria, D-Galactose-induced accelerated aging model: an overview,
546   *Biogerontology*, 2019, **20**, 763-782.
547   4.   T. Takiishi, C. I. M. Fenero and N. O. S. Camara, Intestinal barrier and gut microbiota: Shaping
548   our immune responses throughout life, *Tissue Barriers*, 2017, **5**, e1373208.
549   5.   M. Camilleri, Leaky gut: mechanisms, measurement and clinical implications in humans, *Gut*,
550   2019, **68**, 1516-1526.
551   6.   Y. R. Li, S. Li and C. C. Lin, Effect of resveratrol and pterostilbene on aging and longevity,
552   *Biofactors*, 2018, **44**, 69-82.
553   7.   N. Khan and H. Mukhtar, Tea polyphenols in promotion of human health, *Nutrients*, 2018, **11**,
554   39.
555   8.   S. Hayakawa, T. Ohishi, N. Miyoshi, Y. Oishi, Y. Nakamura and M. Isemura, Anti-cancer effects
556   of green tea epigallocatchin-3-gallate and coffee chlorogenic acid, *Molecules*, 2020, **25**, 4553.
557   9.   M. He, L. Zhao, M. J. Wei, W. F. Yao, H. S. Zhao and F. J. Chen, Neuroprotective effects of (-)-
558   epigallocatechin-3-gallate on aging mice induced by D-galactose, *Biol Pharm Bull*, 2009, **32**, 55-
559   60.
560   10.   Y. Hada, H. A. Uchida, N. Otaka, Y. Onishi, S. Okamoto, M. Nishiwaki, R. Takemoto, H.
561   Takeuchi and J. Wada, The Protective Effect of Chlorogenic Acid on Vascular Senescence via the
562   Nrf2/HO-1 Pathway, *Int J Mol Sci*, 2020, **21**, 4527.
563   11.   Y. Feng, Y. H. Yu, S. T. Wang, J. Ren, D. Camer, Y. Z. Hua, Q. Zhang, J. Huang, D. L. Xue, X. F.
564   Zhang, X. F. Huang and Y. Liu, Chlorogenic acid protects D-galactose-induced liver and kidney
565   injury via antioxidation and anti-inflammation effects in mice, *Pharm Biol*, 2016, **54**, 1027-1034.
566   12.   N. Yamamoto, H. Tokuda, G. Kuroyanagi, S. Kainuma, R. Ohguchi, K. Fujita, R. Matsushima-
567   Nishiwaki, O. Kozawa and T. Otsuka, Amplification by (-)-epigallocatechin gallate and
568   chlorogenic acid of TNF-alpha-stimulated interleukin-6 synthesis in osteoblasts, *Int J Mol Med*,
569   2015, **36**, 1707-1712.
570   13.   L. Yang, L. Jia, X. Li, K. Zhang, X. Wang, Y. He, M. Hao, M. P. Rayman and J. Zhang, Prooxidant
571   activity-based guideline for a beneficial combination of (-)-epigallocatechin-3-gallate and
572   chlorogenic acid, *Food Chem*, 2022, **386**, 132812.
573   14.   A. Ali, S. A. Shah, N. Zaman, M. N. Uddin, W. Khan, A. Ali, M. Riaz and A. Kamil, Vitamin D
574   exerts neuroprotection via SIRT1/nrf-2/ NF-kB signaling pathways against D-galactose-induced
575   memory impairment in adult mice, *Neurochem Int*, 2021, **142**, 104893.
576   15.   T. Shwe, W. Pratchayasakul, N. Chattipakorn and S. C. Chattipakorn, Role of D-galactose-

577   induced brain aging and its potential used for therapeutic interventions, *Exp Gerontol*, 2018, **101**,
578   13-36.

579   16.   Z. Ma, F. Zhang, H. Ma, X. Chen, J. Yang, Y. Yang, X. Yang, X. Tian, Q. Yu, Z. Ma and X. Zhou,
580   Effects of different types and doses of whey protein on the physiological and intestinal flora in
581   D-galactose induced aging mice, *PLoS One*, 2021, **16**, e0248329.

582   17.   J. Kang, Z. Wang, E. Cremonini, G. Le Gall, M. G. Pontifex, M. Muller, D. Vauzour and P. I.
583   Oteiza, (-)-Epicatechin mitigates anxiety-related behavior in a mouse model of high fat diet-
584   induced obesity, *J Nutr Biochem*, 2022, **110**, 109158.

585   18.   Z. Wu, T. Chen, D. Pan, X. Zeng, Y. Guo and G. Zhao, Resveratrol and organic selenium-rich
586   fermented milk reduces D-galactose-induced cognitive dysfunction in mice, *Food Funct*, 2021, **12**,
587   1318-1326.

588   19.   R. Wei, X. Liu, Y. Wang, J. Dong, F. Wu, G. G. Mackenzie and Z. Su, (-)-Epigallocatechin-3-gallate
589   mitigates cyclophosphamide-induced intestinal injury by modulating the tight junctions,
590   inflammation and dysbiosis in mice, *Food Funct*, 2021, **12**, 11671-11685.

591   20.   J. Wang, H. Zhao, K. Lv, W. Zhao, N. Zhang, F. Yang, X. Wen, X. Jiang, J. Tian, X. Liu, C. T. Ho
592   and S. Li, Pterostilbene ameliorates DSS-induced intestinal epithelial barrier loss in mice via
593   suppression of the NF-kappaB-mediated MLCK-MLC signaling pathway, *J Agric Food Chem*,
594   2021, **69**, 3871-3878.

595   21.   J. Qian, X. Wang, J. Cao, W. Zhang, C. Lu and X. Chen, Dihydromyricetin attenuates D-galactose-
596   induced brain aging of mice via inhibiting oxidative stress and neuroinflammation, *Neurosci Lett*,
597   2021, **756**, 135963.

598   22.   J. Liu, D. Chen, Z. Wang, C. Chen, D. Ning and S. Zhao, Protective effect of walnut on d-
599   galactose-induced aging mouse model, *Food Sci Nutr*, 2019, **7**, 969-976.

600   23.   E. Hakimizadeh, M. Zamanian, L. Gimenez-Llort, C. Sciorati, M. Nikbakhtzadeh, M. Kujawska,
601   A. Kaeidi, J. Hassanshahi and I. Fatemi, Calcium dobesilate reverses cognitive deficits and
602   anxiety-like behaviors in the D-galactose-induced aging mouse model through modulation of
603   oxidative stress, *Antioxidants (Basel)*, 2021, **10**, 649.

604   24.   R. Okumura and K. Takeda, Roles of intestinal epithelial cells in the maintenance of gut
605   homeostasis, *Exp Mol Med*, 2017, **49**, e338.

606   25.   T. Finkel and N. J. Holbrook, Oxidants, oxidative stress and the biology of ageing, *Nature*, 2000,
607   **408**, 239-247.

608   26.   M. G. Flynn, M. M. Markofski and A. E. Carrillo, Elevated inflammatory status and increased
609   risk of chronic disease in chronological aging: inflamm-aging or inflamm-inactivity?, *Aging Dis*,
610   2019, **10**, 147-156.

611   27.   A. C. Luissint, C. A. Parkos and A. Nusrat, Inflammation and the intestinal barrier: leukocyte-
612   epithelial cell interactions, cell junction remodeling, and mucosal repair, *Gastroenterology*, 2016,
613   **151**, 616-632.

614   28.   G. Barbara, M. R. Barbaro, D. Fuschi, M. Palombo, F. Falangone, C. Cremon, G. Marasco and V.
615   Stanghellini, Inflammatory and microbiota-related regulation of the intestinal epithelial barrier,
616   *Front Nutr*, 2021, **8**, 718356.

617   29.   M. Serino, E. Luche, S. Gres, A. Baylac, M. Berge, C. Cenac, A. Waget, P. Klopp, J. Iacovoni, C.
618   Klopp, J. Mariette, O. Bouchez, J. Lluch, F. Ouarne, P. Monsan, P. Valet, C. Roques, J. Amar, A.
619   Bouloumie, V. Theodorou and R. Burcelin, Metabolic adaptation to a high-fat diet is associated
620   with a change in the gut microbiota, *Gut*, 2012, **61**, 543-553.

621 30. K. A. Kim, J. J. Jeong, S. Y. Yoo and D. H. Kim, Gut microbiota lipopolysaccharide accelerates
622   inflamm-aging in mice, *BMC Microbiol*, 2016, **16**, 9.
623 31. H. Zhang, Z. Zhang, G. Song, X. Tang, H. Song, A. Deng, W. Wang, L. Wu and H. Qin,
624   Development of an XBP1 agonist, HLJ2, as a potential therapeutic agent for ulcerative colitis, *Eur*
625   *J Pharm Sci*, 2017, **109**, 56-64.
626 32. O. I. Selmin, A. J. Papoutsis, S. Hazan, C. Smith, N. Greenfield, M. G. Donovan, S. N. Wren, T.
627   C. Doetschman, J. M. Snider, A. J. Snider, S. H. Chow and D. F. Romagnolo, n-6 high fat diet
628   induces gut microbiome dysbiosis and colonic inflammation, *Int J Mol Sci*, 2021, **22**, 6919.
629 33. G. Leite, M. Pimentel, G. M. Barlow, C. Chang, A. Hosseini, J. J. Wang, G. Parodi, R. Sedighi, A.
630   Rezaie and R. Mathur, Age and the aging process significantly alter the small bowel microbiome,
631   *Cell Rep*, 2021, **36**, 109765.
632 34. S. M. Lee, N. Kim, J. H. Park, R. H. Nam, K. Yoon and D. H. Lee, Comparative analysis of ileal
633   and cecal microbiota in aged rats, *J Cancer Prev*, 2018, **23**, 70-76.
634 35. E. J. E. Brownlie, D. Chaharlangi, E. O. Wong, D. Kim and W. W. Navarre, Acids produced by
635   lactobacilli inhibit the growth of commensal Lachnospiraceae and S24-7 bacteria, *Gut Microbes*,
636   2022, **14**, 2046452.
637 36. S. Hu, J. Wang, Y. Xu, H. Yang, J. Wang, C. Xue, X. Yan and L. Su, Anti-inflammation effects of
638   fucosylated chondroitin sulphate from Acaudina molpadioides by altering gut microbiota in
639   obese mice, *Food Funct*, 2019, **10**, 1736-1746.
640 37. M. Sibai, E. Altuntas, B. Yildirim, G. Ozturk, S. Yildirim and T. Demircan, Microbiome and
641   longevity: high abundance of longevity-linked Muribaculaceae in the gut of the long-living
642   rodent spalax leucodon, *OMICS*, 2020, **24**, 592-601.
643 38. T. Tavella, S. Rampelli, G. Guidarelli, A. Bazzocchi, C. Gasperini, E. Pujos-Guillot, B. Comte, M.
644   Barone, E. Biagi, M. Candela, C. Nicoletti, F. Kadi, G. Battista, S. Salvioli, P. W. O'Toole, C.
645   Franceschi, P. Brigidi, S. Turroni and A. Santoro, Elevated gut microbiome abundance of
646   Christensenellaceae, Porphyromonadaceae and Rikenellaceae is associated with reduced
647   visceral adipose tissue and healthier metabolic profile in Italian elderly, *Gut Microbes*, 2021, **13**,
648   1-19.
649 39. E. T. Kim, S. J. Lee, T. Y. Kim, H. G. Lee, R. M. Atikur, B. H. Gu, D. H. Kim, B. Y. Park, J. K. Son
650   and M. H. Kim, Dynamic changes in fecal microbial communities of neonatal dairy calves by
651   aging and diarrhea, *Animals (Basel)*, 2021, **11**, 1113.
652 40. W. Turpin, L. Bedrani, O. Espin-Garcia, W. Xu, M. S. Silverberg, M. I. Smith, J. A. R. Garay, S. H.
653   Lee, D. S. Guttman, A. Griffiths, P. Moayyedi, R. Panaccione, H. Huynh, H. A. Steinhart, G.
654   Aumais, L. A. Dieleman, D. Turner, C. I. G. P. r. team, A. D. Paterson and K. Croitoru,
655   Associations of NOD2 polymorphisms with Erysipelotrichaceae in stool of in healthy first degree
656   relatives of Crohn's disease subjects, *BMC Med Genet*, 2020, **21**, 204.
657 41. E. Biagi, L. Nylund, M. Candela, R. Ostan, L. Bucci, E. Pini, J. Nikkila, D. Monti, R. Satokari, C.
658   Franceschi, P. Brigidi and W. De Vos, Through ageing, and beyond: gut microbiota and
659   inflammatory status in seniors and centenarians, *PLoS One*, 2010, **5**, e10667.
660 42. C. J. Anderson, C. B. Medina, B. J. Barron, L. Karvelyte, T. L. Aaes, I. Lambertz, J. S. A. Perry, P.
661   Mehrotra, A. Goncalves, K. Lemeire, G. Blancke, V. Andries, F. Ghazavi, A. Martens, G. van Loo,
662   L. Vereecke, P. Vandenabeele and K. S. Ravichandran, Microbes exploit death-induced nutrient
663   release by gut epithelial cells, *Nature*, 2021, **596**, 262-267.
664 43. K. M. Chasser, K. McGovern, A. F. Duff, B. D. Graham, W. N. Briggs, D. R. Rodrigues, M.

665 Trombetta, E. Winson and L. R. Bielke, Evaluation of day of hatch exposure to various
666 Enterobacteriaceae on inducing gastrointestinal inflammation in chicks through two weeks of
667 age, *Poultry Sci*, 2021, **100**, 101193.
668 44. D. N. Frank, A. L. St Amand, R. A. Feldman, E. C. Boedeker, N. Harpaz and N. R. Pace,
669 Molecular-phylogenetic characterization of microbial community imbalances in human
670 inflammatory bowel diseases, *Proc Natl Acad Sci U S A*, 2007, **104**, 13780-13785.
671 45. J. Cai, L. Zhou, X. D. Song, M. Q. Yin, G. Q. Liang, H. Xu, L. R. Zhang, G. R. Jiang and F. Huang,
672 Alteration of intestinal microbiota in 3-Deoxyglucosone-induced prediabetic rats, *Biomed Res Int*,
673 2020, **2020**, 8406846.
674 46. C. L. Shen, R. Wang, G. C. Ji, M. M. Elmassry, M. Zabet-Moghaddam, H. Vellers, A. N. Hamood,
675 X. X. Gong, P. Mirzaei, S. M. Sang and V. Neugebauer, Dietary supplementation of gingerols-
676 and shogaols-enriched ginger root extract attenuate pain-associated behaviors while modulating
677 gut microbiota and metabolites in rats with spinal nerve ligation, *Journal of Nutritional
678 Biochemistry*, 2022, **100**, 108904.
679 47. C. Khoo, C. Duysburgh, M. Marzorati, P. Van den Abbeele and D. Zhang, A freeze-dried
680 cranberry powder consistently enhances SCFA production and lowers abundance of
681 opportunistic pathogens in vitro, *BioTech (Basel)*, 2022, **11**, 14.
682 48. A. Kaiyrlykyzy, S. Kozhakhmetov, D. Babenko, G. Zholdasbekova, D. Alzhanova, F. Olzhayev,
683 A. Baibulatova, A. R. Kushugulova and S. Askarova, Study of gut microbiota alterations in
684 Alzheimer's dementia patients from Kazakhstan, *Sci Rep*, 2022, **12**, 15115.

685

686

687

688

689

690

691

692

693

694

695

696

697

Figure legends

699

Figure 1. Effect of CGA (C) and EGCG (E) on body weight, food intake and

hepatic functions in D-galactose (M) treated mice. (a) Body weight progression.

Treatment with CGA (C) and EGCG (E) mitigated the body weight loss induced by D-

galactose (M). Results are presented as mean±SD. *p<0.05, **p<0.01 vs. control. (b)

Weekly food intake. Results are presented as mean±SD. (c) Serum levels of Alanine

aminotransferase (ALT) and Aspartate aminotransferase (AST) at euthanasia. Results

are presented as mean±SD.

707

Figure 2. Effect of CGA (C) and EGCG (E), alone and in combination, on the

cognitive performance of mice treated with D-galactose (M). (a) Behavior was

evaluated by the open field test (OFT) and the novel object recognition test (NOR). D-

galactose-treated mice (M) reduced cognitive behavior, which was mitigated by CGA

(C) plus EGCG (E). Results are presented as mean±SD. *p<0.05, **p<0.01 vs. control.

(b) Representative Hematoxylin and Eosin (H&E) histology images of the brain at

euthanasia for all experimental groups. Images at 100x (top) and 400x (bottom)

magnification are displayed. (c) Effect of C and E on p16 and p21 mRNA expression

in D-galactose (M)-treated mice brains. Results are presented as mean±SD. *p<0.05,

**p<0.01 vs. control.

718

719 **Figure 3. CGA (C) and EGCG (E) protected the gut barrier of the mice injured by**

720 **D-galactose (M) treatment.** (a) CGA (C) and EGCG (E) ameliorated the

721 inflammatory cell infiltration induced by D-galactose (M) in colon tissue.

722 Representative H&E histology images of colon tissue at euthanasia for all experimental

723 groups. Images at 40x (top) and 100x (bottom) magnification are displayed. (b) C and

724 E reduced the gut permeability, measured by the fluorescein isothiocyanate-dextran

725 (FITC-Dextran) transport. Results are presented as mean±SD. *$p<0.05$, **$p<0.01$ vs.

726 control. (c) C and E reduced serum endotoxin levels induced by D-galactose. (d) C

727 plus E restored the decrease in tight junction protein expression induced by D-

728 galactose (M) in colon tissue. Immunoblots for zo-1, occludin, and claudin 1 are shown.

729 Loading control: β-actin. Bands were quantified and results are presented as

730 percentage of control. *$p<0.05$ and **$p<0.01$ vs. control. (e) Effect of C and E on colon

731 zo-1, occludin, and claudin 1 mRNA expression in D-galactose (M) treated mice.

732 Results are presented as mean±SD. *$p<0.05$ and **$p<0.01$ vs. control.

733

734 **Figure 4. Effect of CGA (C) plus EGCG (E) on inflammation and gut oxidative**

735 **stress in D-galactose (M) treated mice.** (a) Levels of TNFα, IFN-γ, IL-1β, and IL-6

736 in colon tissues. Results were normalized by protein contents and presented as

737 mean±SD. *$p<0.05$, **$p<0.01$ vs. control. (b) Levels of total antioxidant capacity (T-

738 AOC), malondialdehyde (MDA), and activity of catalase (CAT) and superoxide

739 dismutase (SOD) in colon tissues. Results were normalized by the protein contents

740 and presented as mean±SD. *$p<0.05$, **$p<0.01$ vs. control.

741

Figure 5. Effect of CGA (C) and EGCG (E) on the α-diversity of the fecal microbiome in mice treated with D-galactose (M). Shannon, Simpson, Ace and Chao 1 indexes were determined in Control (Ctrl), D-galactose (M), CGA (C), EGCG (E), and CGA plus EGCG (C+E) groups to evaluate the gut microbiota community diversity and richness among groups. *p<0.05; **p<0.01.

747

Figure 6. Effect of CGA (C) and EGCG (E) on fecal microbiota composition in mice treated with D-galactose (M). (a) Principal coordinates analysis (PCoA) of the community structure. (b) Gut microbiota distribution at the phylum level and the Firmicutes/Bacteroidetes ratio. (c) Gut microbiota distribution at the family level. (d) Community heatmap of relative abundance at the genus level.

753

Figure 7. Linear discriminant analysis effect size (LEfSe) analysis on fecal microbiome of the mice treated with D-galactose (M). Bacterial taxa with linear discriminant analysis (LDA) score>2 specifically enriched in control (Ctrl; red), D-galactose-treated mice (M; blue) and CGA (C) and EGCG (E) (CE; purple) groups.

758

759

760

Figure 1

(a)

(b)

(c)
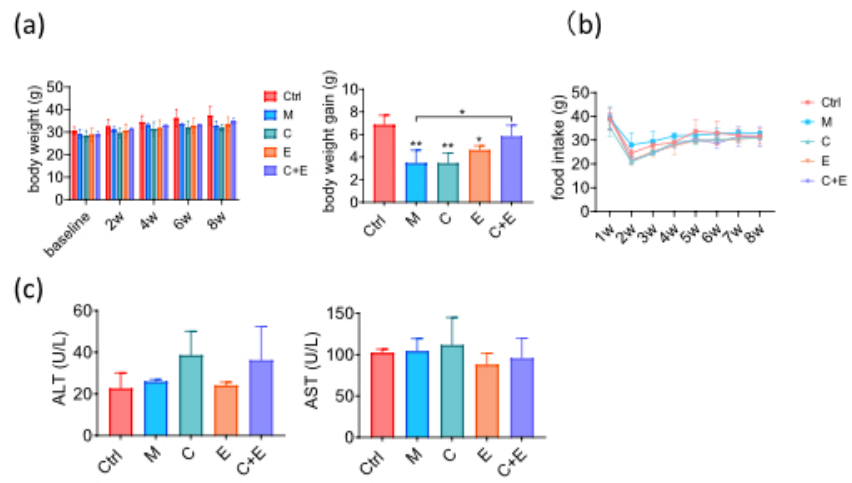
FIgure 1

190x254mm (72 x 72 DPI)

Figure 2
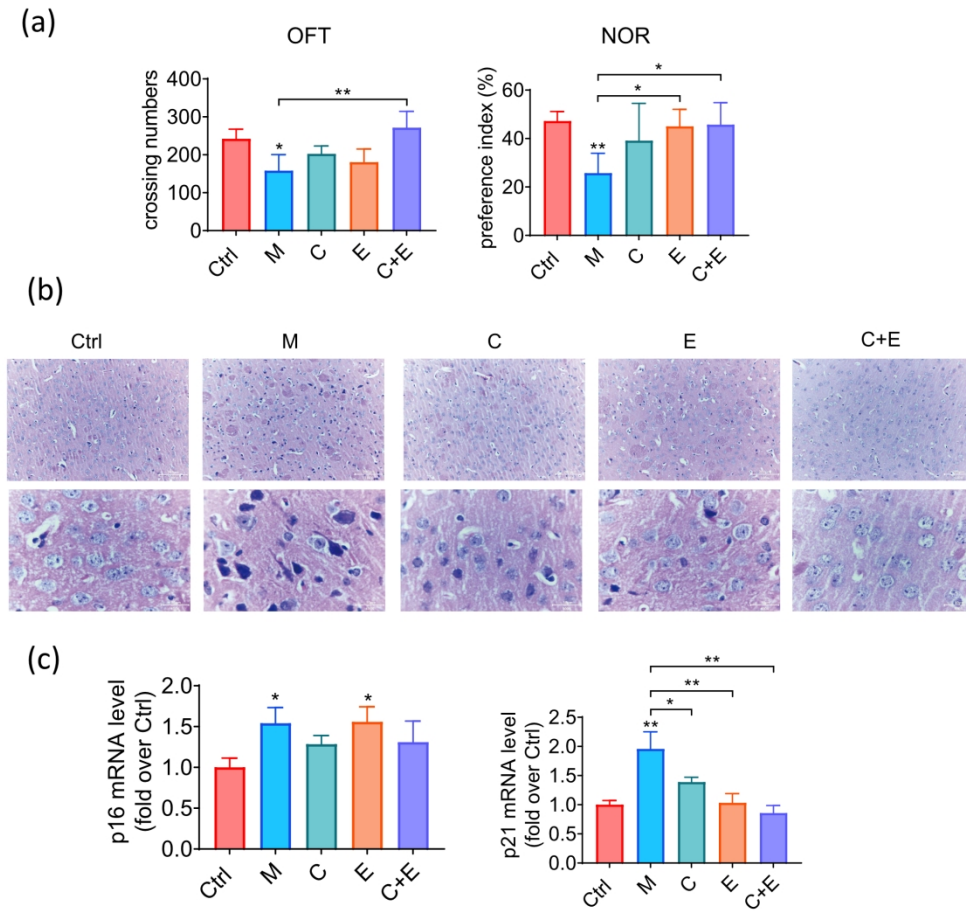
(a)

(b)

(c)

FIgure 2
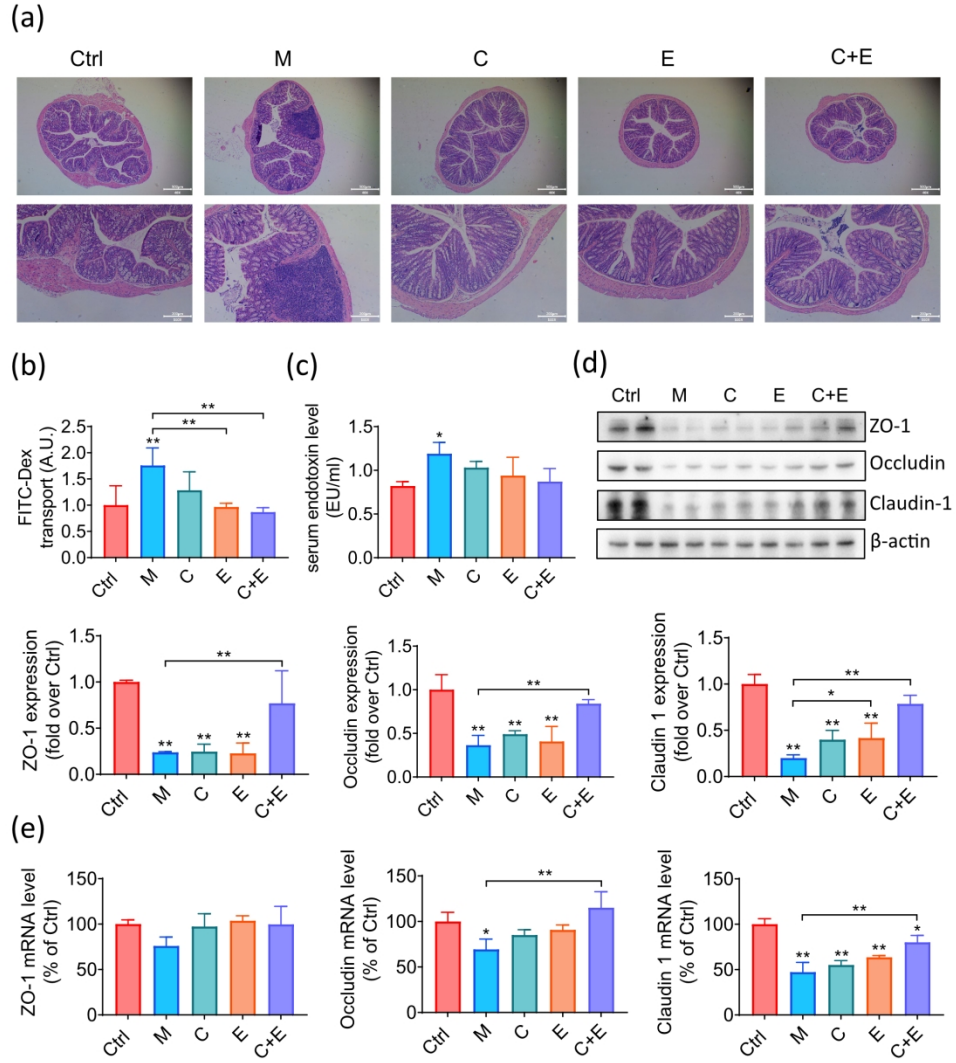
190x205mm (300 x 300 DPI)

Figure 3

Figure 3

190x235mm (300 x 300 DPI)
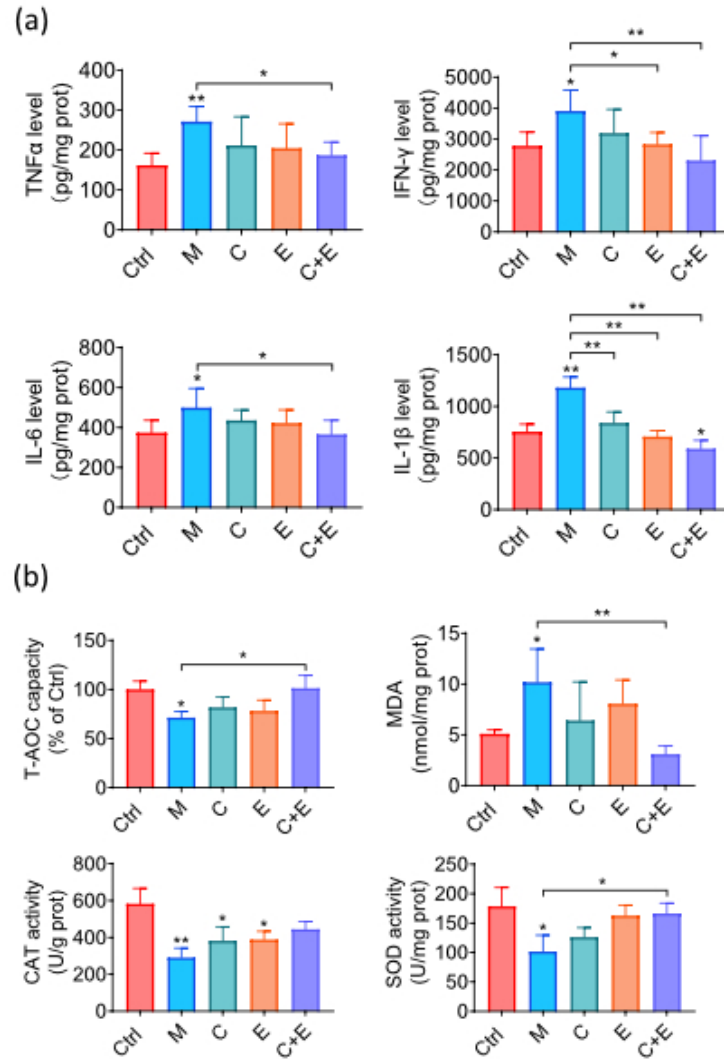
Figure 4

Figure 4

176x233mm (72 x 72 DPI)

Figure 5

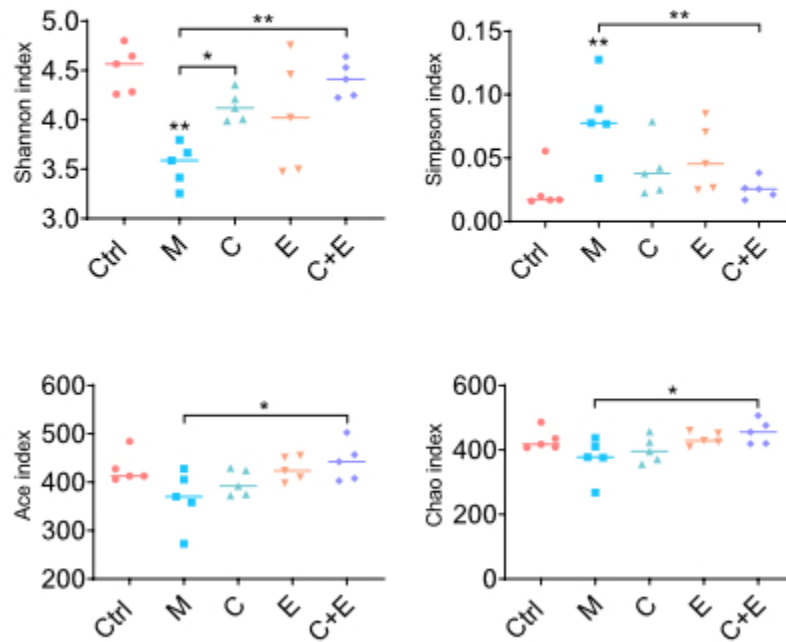Figure 5

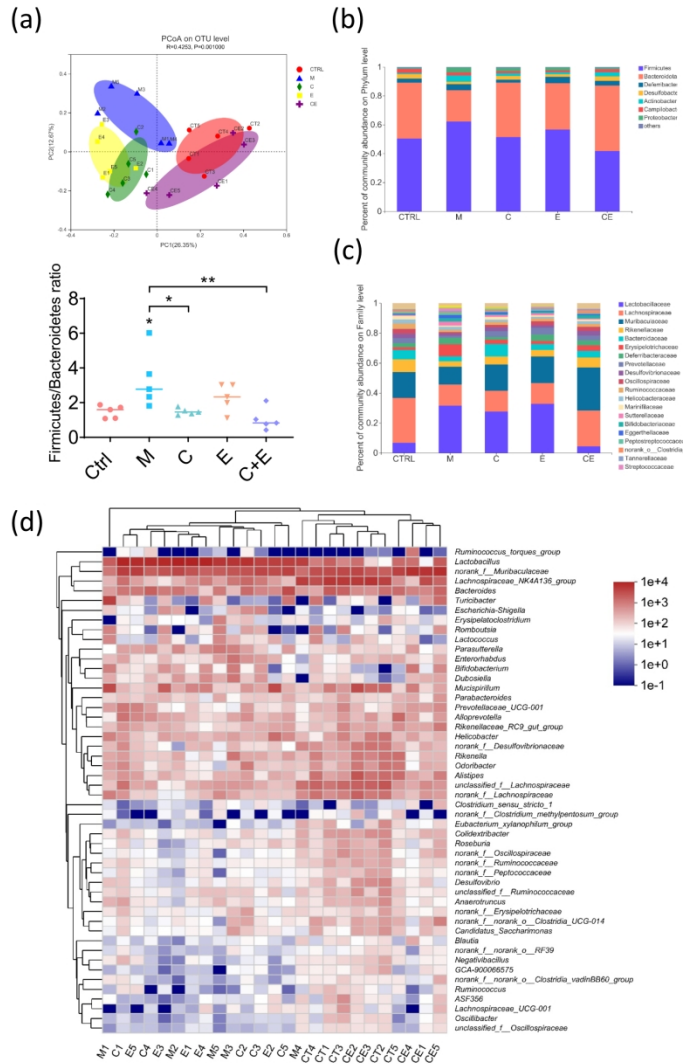174x174mm (72 x 72 DPI)
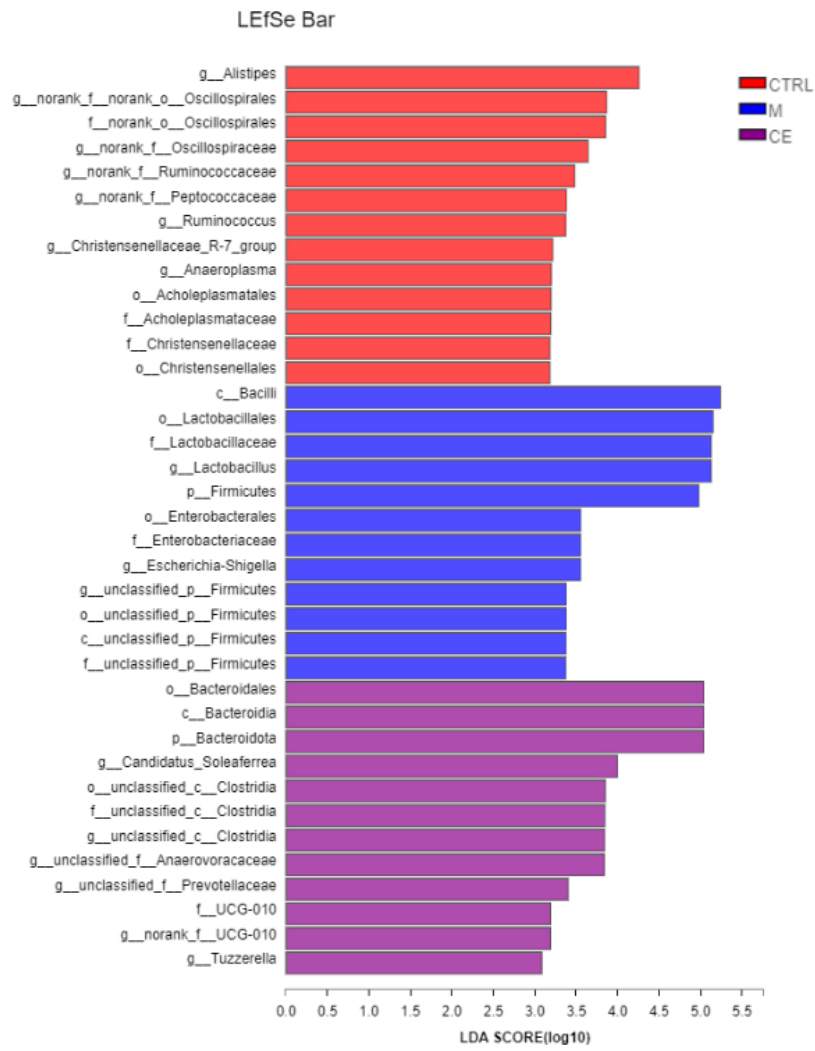
Figure 6

(a)

(b)

(c)

(d)

Figure 6

190x254mm (300 x 300 DPI)

Figure 7

Figure 7

179x227mm (96 x 96 DPI)